Urban Water Journal

ISSN: (Print) (Online) Journal homepage: https://www.tandfonline.com/loi/nurw20

NSGA-II parameterization for the optimal pressure sensor location in water distribution networks

Bruno Ferreira, André Antunes, Nelson Carriço & Dídia Covas

To cite this article: Bruno Ferreira, André Antunes, Nelson Carriço & Dídia Covas (2023) NSGA-II parameterization for the optimal pressure sensor location in water distribution networks, Urban Water Journal, 20:6, 738-750, DOI: 10.1080/1573062X.2023.2209553

To link to this article: https://doi.org/10.1080/1573062X.2023.2209553

Published online: 05 May 2023.

URBAN WATER JOURNAL
2023, VOL. 20, NO. 6, 738–750
https://doi.org/10.1080/1573062X.2023.2209553

Taylor & Francis
Taylor & Francis Group

RESEARCH ARTICLE

NSGA-II parameterization for the optimal pressure sensor location in water distribution networks

Bruno Ferreira [a], André Antunes [b], Nelson Carriço [a] and Dídia Covas [c]

[a]INCITE, ESTBarreiro, Instituto Politécnico de Setúbal, Setúbal, Portugal; [b]Sustain.RD, ESTSetúbal, Instituto Politécnico de Setúbal, Setúbal, Portugal; [c]CERIS, Instituto Superior Técnico, Universidade de Lisboa, Lisbon, Portugal

ABSTRACT

The optimal location of pressure sensors is typicallysolved using heuristic algorithms. Non-dominated Sorting Genetic Algorithm II (NSGA-II) is one of the most used algorithms in the water industry, requiring a preliminary parameter tuning process. The lack of guidelines on how to tune model parameters generally limits the use of these algorithms by researchers or practitioners and, as such, fails to be used in real-life problems. The current paper explores different NSGA-II parameterizations for the optimal location of pressure sensors by using a multi-objective optimization methodology applied to a real distribution network. Results show that (i) both the uniform and simulated binary crossover operators (depending on the internal parameters) produce the best results, being the former recommended since it does not require further parameter tuning; (ii) polynomial mutation with lower probability value should be chosen; and (iii) the distribution indices of polynomial mutation have a minor effect on NSGA-II performance.

ARTICLE HISTORY
Received 9 February 2022
Accepted 21 April 2023

KEYWORDS
Hypervolume; multi-objective; NSGA-II; optimization; pressure sensors

1. Introduction

Water distribution networks (WDNs) are important public infrastructures to ensure water supply and delivery to populations in quantity and with acceptable quality and pressure. In developed countries, most WDNs were built several decades ago, having, nowadays, high levels of water losses and frequent pipe bursts due to the inevitable ageing and deterioration process associated with intensive use (Leitão et al. 2016). In this context, collecting and processing pressure and flow rate data play an important role in the daily operation of WDNs as these carry information about the actual condition and performance of these systems. Such data can be used with advanced machine learning and optimization techniques in different frameworks of hydraulic engineering and water resources analysis. Salloom, Kaynak, and He (2021) used deep learning techniques for short-term water demand forecasting. Vonk, Cirkel, and Blokker (2019) used a machine learning model to estimate the peak daily water demand under distinct climate change and vacation scenarios. Menke et al. (2016) explored the optimal pump scheduling to improve energy efficiency and shift electricity consumption to low-tariff periods. Gomes, Vinga, and Henriques (2021) analyzed the time-varying pairwise correlations between pressure sensors for anomaly detection.

Pressure and flow rate data are widely used in the calibration process of highly uncertain variables of hydraulic models, such as nodal demands and pipe roughness coefficients (Dini and Tabesh 2014; Do et al. 2016; Kumar, Narasimhan, and Bhallamudi 2010; Meirelles et al. 2017; Zhang et al. 2018). Only a well-calibrated hydraulic model can be reliably used to detect and locate leaks and pipe bursts by inverse analysis (Hajibandeh and Nazif 2018; Moasheri and Jalili-Ghazizadeh 2020), by using a classifier approach (Capelo et al. 2021; Fereidooni, Tahayori, and Bahadori-Jahromi 2021; Hu et al. 2021; Rayaroth and G 2019), or by using error domain model falsification approach (Goulet, Coutu, and Smith 2013; Moser, Paal, and Smith 2018). Pressure data used for model calibration and burst detection are collected using sensors installed in the WDN. However, only a limited number of sensors can be installed in a WDN due to budget constraints. This leads to the question of where and how many pressure sensors should be installed to maximize the total benefit and reduce the associated costs.

Many methodologies based on different principles have been developed to optimally locate pressure sensors in WDNs. Simone, Giustolisi, and Laucelli (2016) located the pressure sensors based on the network topological analysis; the WDN is divided into distinct zones and a pressure sensor is located in each zone centroid. In Klapcsik, Varga, and Hős (2017), the graph theory is used to divide the WDN into subsystems, and the choice of locating single or several sensors per subsystem is made at a higher level. In a different approach, Cao et al. (2019) locate the sensors in order to represent the different pressure patterns of homogeneous areas of the WDN. The maximization of the accuracy of the hydraulic model is considered by Kapelan, Savic, and Walters (2005) and Behzadian et al. (2009). More recently, Francés-Chust et al. (2020) considered the maximization of nodal pressure sensitivities. Related to leak and pipe burst-detection, Casillas et al. (2013) and Steffelbauer and Fuchs-Hanusch (2016) aim at maximizing the percentage of leak scenarios correctly identified

CONTACT Bruno Ferreira bruno.s.ferreira@estbarreiro.ips.pt

(according to certain criteria), while in Sarrate et al. (2014) the aim is to maximize the leak detectability. Raei et al. (2019) focused on reducing the time of pipe burst event detection, while Zhao et al. (2020) maximize the detection coverage. Hu et al. (2021) located the pressure sensors for pipe burst detection using a hierarchical algorithm that allowed the consideration of sensor-failure scenarios.

Ferreira, Carriço, and Covas (2021, 2022) proposed a multi-objective optimization method for determining the optimal number and location of pressure sensors considering both the hydraulic model calibration and pipe burst detection. Several optimization problems (for a distinct number of pressure sensors) are solved and the hypervolume quality measure (Auger et al. 2009), which evaluates the benefit of installing each number of sensors, is computed for each resulting Pareto front. The optimal number of pressure sensors is determined by assessing the evolution of the hypervolume with the number of sensors. The NSGA-II heuristic algorithm (Deb et al. 2002) is used to solve the multi-objective optimization problem. This algorithm requires specific parameters to be tuned for better performance. The lack of guidelines on how to tune those specific parameters limits the use of such methods by researchers and practitioners and, as such, fails to be used in real-life problems (Wang et al. 2019).

The current paper is the follow-up of the research developed by Ferreira, Carriço, and Covas (2021, 2022). First, the paper explores different NSGA-II parameterizations, specifically tailored to the optimal location of pressure sensor problem. The problem is applied to a real case study located in Lisbon metropolitan area, Portugal. An extensive analysis of the evolution of the hypervolume indicator (Auger et al. 2009) is carried out for different combinations of NSGA-II parameters. An optimal set of NSGA-II parameters is obtained that can be used in similar optimal pressure sensor location problems. Secondly, the paper compares and discusses the results obtained by using two different quality measures – the hypervolume (Auger et al. 2009) and an adaptation of the generational distance (Van Veldhuizen 1999) – to assess their effectiveness in the determination of the optimal location of sensors.

The main novel contributions of this research work are as follows: (i) the summary of lessons learned in the tuning process of NSGA-II parameters for the optimal location of pressure sensors; (ii) the discussion of results obtained by using two quality measures to assess the total benefit of a certain number of pressure sensors and the respective effect on the optimal number of pressure sensors; and (iii) the demonstration of the analysis using a real case study with more than 1000 nodes.

2. Methods

2.1 Optimal location of pressure sensors

Different methodologies can be used to determine the optimal location of a given number (N) of pressure sensors in a WDN. This paper follows the methodology proposed in Ferreira, Carriço, and Covas (2021, 2022) which focuses on pressure sensor location for a better calibration of the hydraulic network model and a more reliable near real-time detection of sudden pipe bursts.

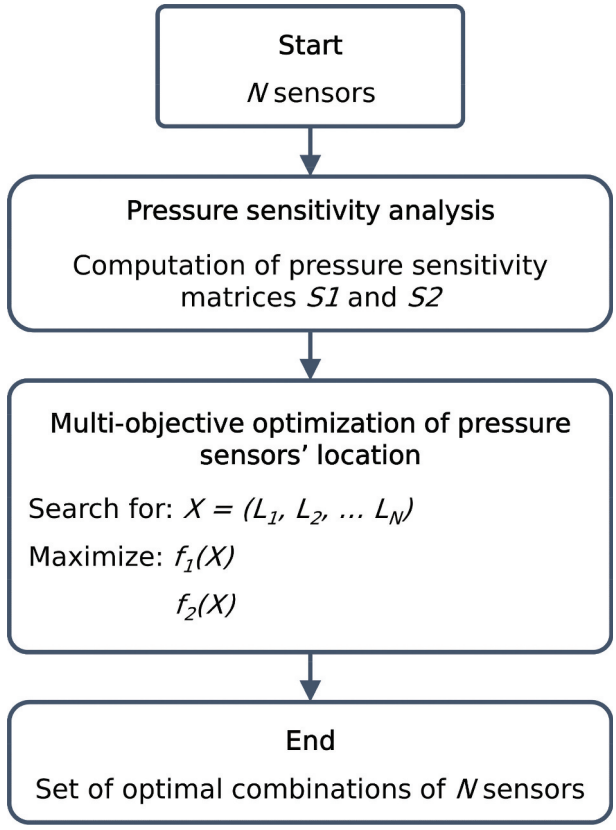

Figure 1. Sequence of steps to obtain a set of optimal combinations of N pressure sensors.

The methodology steps are depicted in Figure 1 and include the formulation of an unconstrained multi-objective optimization problem in which the decision variables are the N nodes where the pressure sensors could be potentially installed. Pressure sensors are optimally located based on the maximization of nodal sensitivities for both pipe roughness coefficients and pipe burst sizes. The calculation of the objective function (OF) requires the prior computation of two pressure sensitivity matrices, namely, one for the pipe roughness coefficient ($S1$) and the other for the pipe burst size ($S2$). The matrices assess changes in nodal pressure-head values due to variations in pipe roughness coefficients and pipe burst sizes (simulated by the nodal emitter coefficient). For a given network with N_p pipes and N_n nodes, the sizes of the obtained matrices $S1$ and $S2$ are $N_p \times N_n$ and $N_n \times N_n$, respectively. Matrix component $S1_{i,j}$ refers to the variation of the pressure-head in node j given the variation of the pipe roughness coefficient of pipe i. Similarly, $S2_{i,j}$ refers to the variation of the pressure-head in node j for the variation in the pipe burst size in node i. These matrices can be numerically calculated by a finite difference scheme whose terms are obtained by hydraulic simulations (see the original research paper by Ferreira et al. 2022 for more details on the pressure sensitivity analysis). More advanced techniques for pressure sensitivity analysis (Kapelan, Savic, and Walterrs 2007; Liggett and Chen 1994) could be used; however, these are not easily applicable to real-case studies (Pérez et al. 2011).

Two distinct OFs are considered for the formulation of the multi-objective optimization problem for a given sampling

design X. A sampling design X is a discrete set of N pressure sensors. The first function, f_1, aims at maximizing the sensitivity to the pipe roughness coefficient covered by sampling design X. This OF can be computed as follows:

$$Maximize\, f_1(X) = \sum_{i=1}^{Np} a_i, where\, a_i = \max_{j \in X} \left(S1_{i,j}\right) \quad (1)$$

where N_p is the number of pipes.

A second function, f_2, aims at maximizing the sensitivity of the sampling design X to pipe burst events and can be computed as follows:

$$Maximize\, f_2(X) = \sum_{i=1}^{Nn} a_i, where\, a_i = \max_{j \in X} \left(S2_{i,j}\right) \quad (2)$$

where N_n is the number of nodes.

As noted by Ferreira et al. (2022), both S1 and S2 sensitivity matrices are not perfectly correlated and, as such, different optimal combinations of sensors can be found for solutions f_1 and f_2. Thus, the result of the optimization problem is a set of optimal combinations of N sensors, also known as a Pareto front. Each solution of the Pareto front represents a specific combination of N sensors (characterized by the values of f_1 and f_2), for which no other combination exists (with N sensors) that presents better results for both objectives. The fact is that differences can be found in the performance of pipe roughness calibration and pipe burst location by using either the solution maximizing f_1, f_2, or the trade-off solution (as demonstrated in Ferreira et al. 2022).

By solely considering the maximization of sensitivities, there is an inherent risk that the optimal solution leads to sensors clustered in zones with highly sensitive nodes. As demonstrated further in this paper, a trade-off solution between objectives f_1 and f_2 has the ability to minimize the effect of such clustered sensors and guarantee the spread of sensors in the WDN. The f_1 and f_2 values of each optimal combination of N sensors will be used to assess the benefit of installing N sensors in the WDN (as further explained in 2.3).

2.2 Investigation of the NSGA-II parameterization

The unconstrained multi-objective optimization problem presented in 2.1 can be solved by using different heuristic techniques, namely, multi-objective genetic algorithm (Fonseca and Fleming 1993), multi-objective particle swarm optimization (Coello Coello and Lechuga 2002), or non-dominated sorting genetic algorithm II (NSGA-II) (Deb et al. 2002), among others. This paper uses the NSGA-II since it is considered to be an 'industry standard' (Wang et al. 2019) and has been successfully applied to a variety of water resource optimization problems (Maier et al. 2014; Mala-Jetmarova, Sultanova, and Savic 2018; Reed et al. 2013). This algorithm ranks the solutions based on the Pareto dominance relationship and a sorting criterion known as crowding distance. Solutions with higher rankings and larger crowding distances survive and are selected to reproduce across generations.

The NSGA-II has different parameters that strongly affect the computational efficiency (convergence velocity) and effectiveness (success in finding the optimal solution) that should be carefully tuned and tested to take full advantage of the method's capabilities (Wang et al. 2019). As noted by the 'No Free Lunch' theorem (Wolpert and Macready 1997), a group of parameters cannot be found that is always effective across different optimization problems. In other words, a set of highly effective parameter values matching NSGA-II capabilities to the characteristics of the optimal pressure sensor location problem should exist.

The following parameters are considered for tuning: 1) the population size (PS), 2) the number of generations (NG), 3) the crossover operator and 4) the mutation operator. The first two parameters (PS and NG) determine together the computation effort applied to a given problem, since PS × NG equals the total number of evaluations. A larger NG normally ensures better convergence, but the convergence rate significantly declines as NG increases. Furthermore, the PS is essential to ensure convergence, as an inadequately small value can lead to a population with similar solutions (rather than a diversified set of solutions).

The third parameter to be tuned is the crossover operator. Different crossover operators can be used, namely, simulated binary (SB), uniform and half-uniform, one-point and two-point, and exponential crossover, among others. In SB, the real values are represented by a binary notation, and the working principle of the single-point crossover operator on binary strings is carried with a given probability p_c. The exponential distribution of probabilities can be fine-tuned by using the distribution indices n_c. More details regarding the SB crossover operator can be found in Deb, Sindhya, and Okabe (2007). The uniform crossover takes with a probability of 0.5 the values from each parent (not a sequence of values but one value at a time). In the half-uniform crossover, the different values in the first and second parents are first selected. Then, half of the different values in each parent are randomly selected. The one-point crossover works by randomly selecting one point in both the parents, thus leaving the offspring with a sequence of values from both parents. The two-point crossover works similarly but by considering two random points. Finally, the exponential crossover is mainly a one-point crossover that may occasionally perform as a two-point crossover, and which can be tuned with the probability parameter p. Note that some crossover operators (SB and exponential crossover) have internal parameters, such as the probability of crossover p_c and distribution indices n_c in SB and probability p in exponential crossover operator.

The fourth parameter to be tuned is the mutation operator. The polynomial mutation is used (with its associated probability of mutation p_m and distribution indices n_m). This operator works by mutating the individual values of each population member after a crossover with a given probability, p_m. The distribution of probabilities can be fine-tuned by using the distribution indices, n_m.

In this study, random sampling and selection methods are used. These parameters do not require any tuning. So, multiple NSGA-II combinations of parameters can be generated by varying the PS, NG, the crossover and the mutation operator.

The tuning process is performed by considering an initial estimation of the NSGA-II parameters (see Table 1) based on previously published research (Wang et al. 2019). This initial estimation of the NSGA-II parameters is used for the optimal design of WDNs, which involves a distinct multi-

Table 1. Initial estimation of NSGA-II parameters.

Parameter	Initial estimation
Population Size (PS)	100
Number of generations (NG)	100
Crossover operator	Simulated binary (p_c=0.95; n_c=10)
Mutation operator	Polynomial mutation (p_m=0.05; n_m=10)

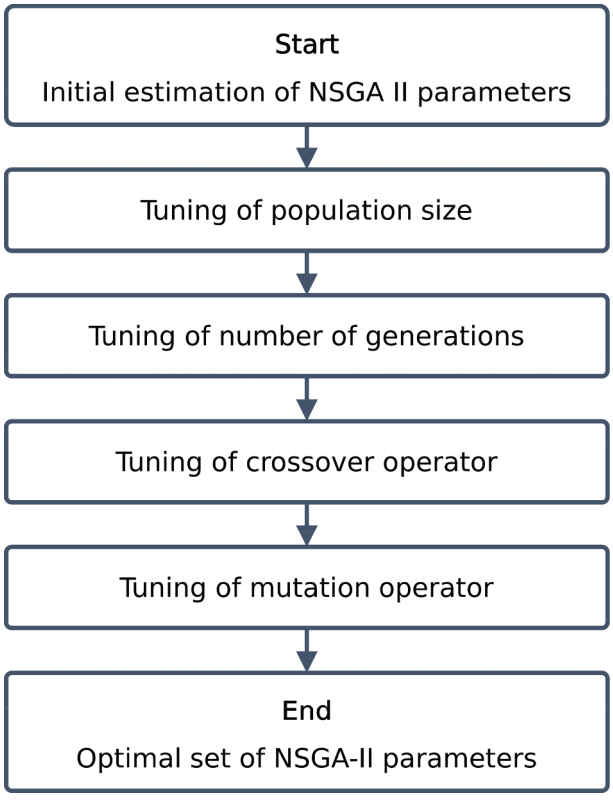

Figure 2. Sequence of steps for the NSGA-II parameterization.

objective formulation. Thus, these parameters may not be optimized for the problem of the optimal location of pressure sensors.

Figure 2 depicts the general steps for the parameterization of NSGA-II. The following tuning process is performed for each parameter:

(1) Multiple alternatives are considered for the parameter being tuned (e.g. a PS of 50, 100, and 250). The remaining parameters should be considered as in Table 1 or, if available, the tuned values.
(2) The unconstrained multi-objective optimization problem (see 2.1) is solved for a given number of N sensors using the NSGA-II with each parameter alternative. The hypervolume indicator (Auger et al. 2009) is used to assess the evolution of the Pareto front across the generations and, thus, the performance of each alternative of parameters.
(3) The best parameter alternative is chosen, and the next parameter can be tuned.

Parameters like the crossover and mutation operators may result in a large number of alternatives as more than one internal value can be affected. For instance, SB leads to nine alternatives when considering three values for both p_c and n_c.

2.3 Determination of the optimal number of pressure sensors using a quality measure

A cost–benefit analysis (CBA) is used to determine the optimal number of sensors, N_{opt}. This step is based on Zhao et al. (2020) who have originally used CBA to determine the optimal number of pressure sensors for burst detection that resulted from the best relation between the benefit and the respective cost.

The minimum and the maximum number of sensors that can be installed in the network, N_{min} and N_{max}, should be first established. These limits define the decision space where the optimal number of sensors will be searched. The N_{min} is equal to one, since at least one sensor will be installed, while the N_{max} may be established based on different criteria, such as the available budget (Behzadian et al. 2009; Quintiliani et al. 2020), the number of possible locations (Raei et al. 2019), or the network size (Steffelbauer and Fuchs-Hanusch 2016).

The total expenditure (TOTEX) associated with N sensors comprises, generally, the capital expenditure (CAPEX) and the annual operation and maintenance expenditures (OPEX) of those sensors. The CAPEX of a single pressure sensor is usually related to its accuracy and the coupled transmission or logging equipment (Zhao et al. 2020). In this study, it is assumed that the total expenditure (TOTEX) associated with the N pressure sensors, *TOTEX(N)*, can be described as follows:

$$TOTEX(N) = C_{unit} \times N \tag{3}$$

where C_{unit} is the unit cost of a pressure sensor including the CAPEX and OPEX and N is the total number of sensors to be installed.

The benefit of installing a certain number of N pressure sensors can be given by the quality of the Pareto front related to that number of sensors (Ferreira, Carriço, and Covas 2021). So, the optimization problem presented in 2.1 should be solved for each N in the range of N_{min} and N_{max}, resulting in a Pareto front for each number of sensors. The goal is to assess the total benefit associated with each number of sensors, i.e. to obtain a single value that represents the quality of each Pareto front. In this paper, two quality measures are used, namely, the hypervolume (Auger et al. 2009) and an adaptation of the generational distance (Van Veldhuizen 1999) indicators.

The hypervolume indicator is described as the 'volume' (defined in as many dimensions as the number of OFs) of the objective space dominated by the Pareto front and delimited by a reference point. In this study with two OFs, the hypervolume indicator describes the 'area' dominated by the set of optimal solutions according to objectives f_1 and f_2. The main

advantages of this metric are the simplicity and the properties related to guaranteeing strict monotonicity regarding Pareto dominance (Guerreiro, Fonseca, and Paquete 2020). Furthermore, it can capture the spread of the solutions across the objective space to some extent. Nonetheless, it may be sensitive to the extreme points of the Pareto front (While et al. 2006). The formal mathematical formulation for the hypervolume indicator is presented in Guerreiro, Fonseca, and Paquete (2020). Figure 3(a) depicts the hypervolume for two Pareto fronts relative to N and $N+1$ sensors; the solutions of the Pareto fronts are depicted in circular blue and orange markers, respectively. The hypervolume is represented as a blue cross-pattern and orange area for N and $N+1$ sensors. The chosen reference point is the origin (0,0) since both objectives aim at the maximization of the OF. The benefit of using $N+1$ sensors (which is naturally higher than the benefit for N sensors) is represented by a higher hypervolume value (i.e. the orange area is larger than the blue cross-pattern area).

The generational distance measures the average Euclidean distance from any point in the obtained Pareto front to the closest point in the true Pareto front. The true Pareto front represents the globally non-dominated set of solutions. As noted by Laszczyk and Myszkowski (2019), the true Pareto front in real-world problems is often unknown. In these situations, reference points can be used. The mathematical formulation for the generational distance can be found in Van Veldhuizen (1999). It is a straightforward measure to compute, although it might be sensitive to the number of points in the Pareto front (Audet et al. 2021) and, unlike the hypervolume indicator, does not capture the spread of the solutions across the objective space. An adaptation of the generational distance is used herein by considering a reference point (0,0) and by calculating the average Euclidean distance between each point of the Pareto front and the reference point. These distances are represented in Figure 3(b) in dashed blue and orange lines (for N and $N+1$ sensors, respectively). Note that the benefit for $N+1$ sensors is represented by a higher average line's length (in orange lines) when compared to those related to N sensors (in blue lines). Since both OFs present distinct units, a normalization process is carried out for the f_1 and f_2 values of each solution of the Pareto front before computing the Euclidean distances. For this purpose, f_1^{max} and f_2^{max} are calculated by considering that a sensor is installed in each possible location. The f_1^{min} and f_2^{min} are considered equal to zero (since both objectives aim at maximization). Accordingly, the normalized values of function f_i of each solution are calculated as follows:

$$f_i^{norm} = \frac{f_i - f_i^{max}}{f_i^{max} - f_i^{min}} \tag{4}$$

The total benefit associated with a given number of sensors N is either described by the respective hypervolume or the generational distance. So, HV and GD are the sets of hypervolume, and generational distance values obtained from each of the Pareto fronts between N_{min} and N_{max}. $HV(N)$ and $GD(N)$ refer to the hypervolume and generational distance, respectively, related to N sensors.

Since both units (benefit and cost units) differ, a normalization of the previously obtained sets $TOTEX$, HV, and GD to [0,1] is required. This leads to the normalized set of installation cost $TOTEX_{norm}$, as well as the normalized sets of hypervolume and generational distance values, HV_{norm} and GD_{norm} (which describe the benefit). The normalized values can be computed as follows:

$$TOTEX_{norm}(N) = \frac{TOTEX(N) - TOTEX(N_{min})}{TOTEX(N_{max}) - TOTEX(N_{min})} \tag{5}$$

$$HV_{norm}(N) = \frac{HV(N) - HV(N_{min})}{HV(N_{max}) - HV(N_{min})} \tag{6}$$

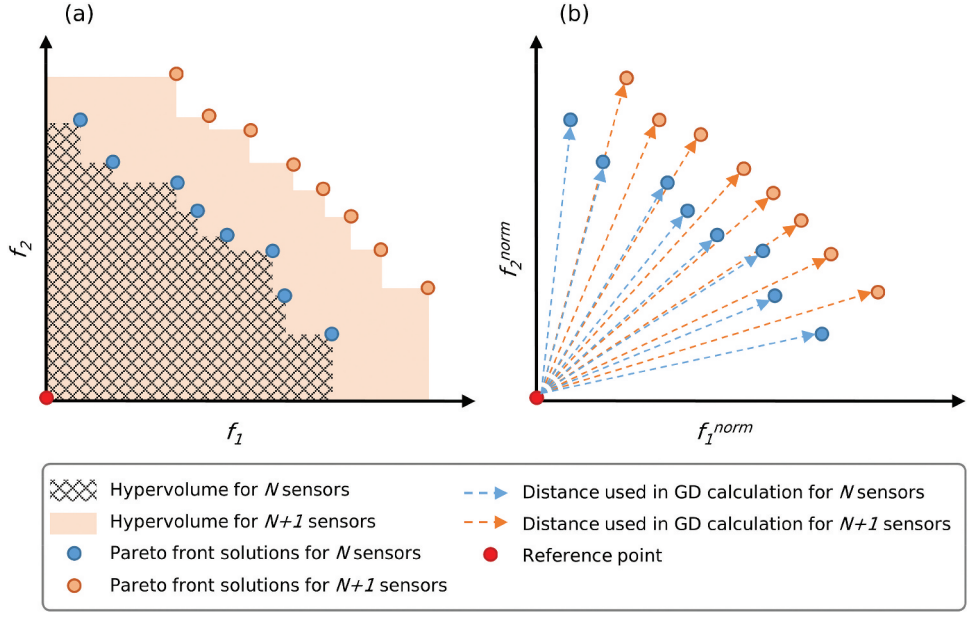

Figure 3. Assessment of the total benefit for a given number of sensors using: (a) the hypervolume and (b) the generational distance.

$$GD_{norm}(N) = \frac{GD(N) - GD(N_{min})}{GD(N_{max}) - GD(N_{min})} \quad (7)$$

where $TOTEX_{norm}(N)$ is the normalized total cost for N sensors, and $HV_{norm}(N)$ and $GD_{norm}(N)$ are, respectively, the normalized hypervolume and generational distance values for N sensors.

By considering that C_{unit} is the same regardless of the number of sensors N, the $TOTEX_{norm}$ calculation could be simplified as follows:

$$TOTEX_{norm}(N) = \frac{C_{unit} \times N - C_{unit} \times N_{min}}{C_{unit} \times N_{max} - C_{unit} \times N_{min}} = \frac{N - N_{min}}{N_{max} - N_{min}} \quad (8)$$

Finally, the relationship between the benefit and the cost of installing the distinct number of sensors can be assessed. To this end, the final net cost for a given number of sensors, $NC(N)$, is computed as the difference between the benefit, described by the $HV_{norm}(N)$ or by the $GD_{norm}(N)$, and the real cost, described by the $TOTEX_{norm}(N)$:

$$NC_{HV}(N) = HV_{norm}(N) - TOTEX_{norm}(N) \quad (9)$$

$$NC_{GD}(N) = GD_{norm}(N) - TOTEX_{norm}(N) \quad (10)$$

where $NC_{HV}(N)$ is the final net cost for a given number of N sensors when using the hypervolume to characterize the total benefit and the $NC_{GD}(N)$ represents the final net cost by using the generational distance to characterize the total benefit.

The optimal number of sensors N_{opt} can be determined by analyzing the relationship between the final net cost and the number of sensors, specifically as the number of sensors with maximum net cost value.

In a real WDN, the total capital cost for installing pressure sensors may not increase linearly with the number of sensors, as typically the unit cost, C_{unit}, is demonstrated to decrease with the increase in the number of sensors. Such non-linear costs can be included in the analysis by changing the *TOTEX* calculation. The comparison of how linear and non-linear cost functions affect the optimal number of pressure sensors using cost–benefit analysis is out of the scope of this study and can be carried out in future works.

3. Application to a case study: results and discussion

3.1 Case study description

The case study is a real WDN located in the Lisbon metropolitan area, Portugal, that supplies approximately 700,000 m^3/year of water to a population of 14,000 inhabitants. The supplied area spans 4 km^2 and is quite heterogeneous in terms of buildings' typology and functionality containing residential buildings as well as a few supermarkets, schools, a large sports complex, a central hospital, some shops, and industrial plants. The WDN has an approximate length of 36 km with about 2,200 service connections. Most pipes are made of asbestos cement (63%), PVC (34%), and HDPE (3%), with diameters ranging from 32 to 400 mm. The hydraulic model, developed in EPANET, includes 967 pipes and 1,262 nodes. The network is supplied by one storage tank with a pumping station. The pumping station is set to operate at a constant pressure throughout the day and is simulated as a constant-level tank (reservoir). Also, 24-h consumption patterns are included in the hydraulic model, allowing extended period simulations. Table 2 summarizes the characteristics of the WDN.

Figure 4(a) presents the analysed WDN with the location of the storage tank (in blue square marker), the diameter of each pipe (given by the colour of each pipe), and the location of the three largest consumers (in blue, orange, and green triangular markers). The three largest consumers

Table 2. A summary of the characteristics of the case study.

Supplied area		4 km^2
Total length		36 km
Number of service connections		2,200
Type of users		Heterogeneous, with residential, commercial, and industrial users
Inlet of the WDN		1 storage tank upstream of a pumping station
Average flow rate at the inlet		30 L/s
Pipe diameters		32 to 400 mm
Pipe materials		Asbestos cement (~63%), PVC (~34%) and HDPE (~3%)
Supplied volume per year		700,000 m^3
Supplied population		14,000 inhabitants
Hydraulic model	Number of nodes	1,262 nodes
	Number of pipes	967
	Extended period simulations	24 periods of average hourly consumption

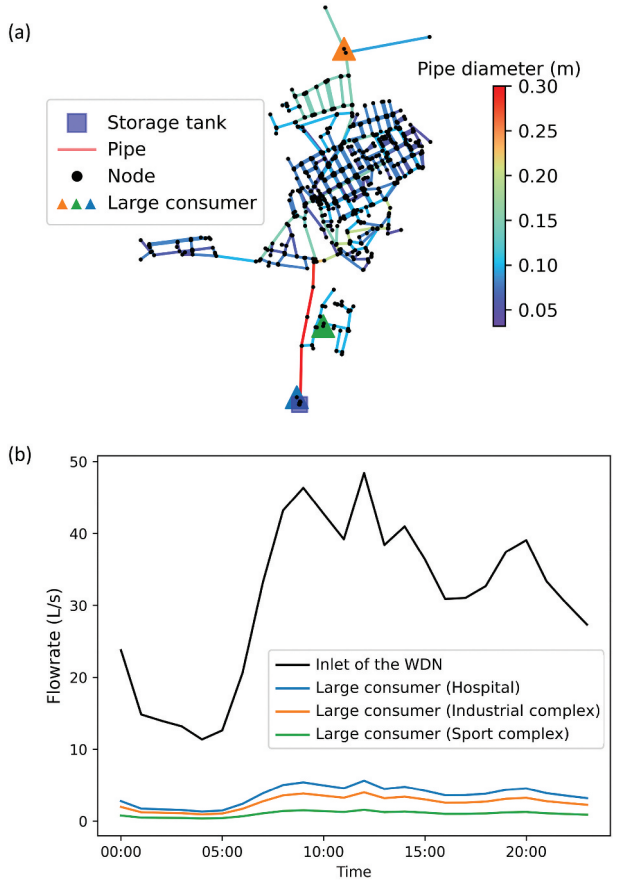

Figure 4. (a) WDN with information on the pipe diameter and the location of the three largest consumers; (b) average daily consumption of the three largest consumers and inlet flow rate of the WDN.

are a hospital, an industry, and a sports centre, with an average daily consumption of 3.60, 2.55, and 1 L/s, respectively. The average daily consumption of the largest consumers is presented in Figure 4(b), as well as the inlet flow rate of the WDN.

The optimization problem related to pressure sensor location in the WDN often results in a large search space, as thousands of nodes can be potential locations for pressure sensors. For the analyzed network with 1,262 nodes, 2.72×10^{24} different combinations of 10 pressure sensors can be found. Many of these 1,262 nodes are redundant and irrelevant for the analysis since they represent similar locations in the network. In this paper, a search space reduction process (i.e. the reduction of the number of node candidates to sensor location) is carried out aiming at reducing the number of possible combinatorial solutions of sensor locations. The search space reduction process is carried out as described in Sophocleous, Savić, and Kapelan (2019) by excluding all nodes associated with non-pipe components. These nodes are only excluded from the range of candidate locations but continue to exist in the hydraulic model. This model has 390 valves that are spread across the network. By applying the search space reduction, the number of possible sensor locations is reduced from 1,262 to just 481, since upstream and downstream nodes of valves are excluded, as well as the storage tank node. As such, there are 1.66×10^{20} different combinations of 10 pressure sensors (considering 481 possible locations), which corresponds to a reduction factor of about 16,000 in the search space for this number of sensors.

A pressure sensitivity analysis is carried out by considering a variation on the Hazen-Williams's pipe roughness coefficient of 10 and by generating a burst of a fixed size for every node of the hydraulic model with a single emitter coefficient of 0.0002 $m^{2.50}/s$ and an emitter exponent of 0.5 (leading to an average burst of 1 L/s for an average pressure-head of 30 m). The hydraulic simulations are carried out with the EPANET toolkit (Rossman 2000) within the Water Network Tool for Resilience (WNTR) Python package (Klise et al. 2017). Extended period simulations are considered in the calculation of each pressure sensitivity matrix; one matrix was calculated for each time step and the mean values are calculated to obtain the final matrices *S1* or *S2*.

3.2 Problem formulation and NSGA-II parameterization

The optimization problem is formulated in NSGA-II using discrete variables and integer encoding; each discrete location (i.e. node) is assigned an integer value. A population member is a set of locations for the pressure sensors (set of integer values) and each variable of a population member represents a possible pressure sensor location (a single integer value). A repair algorithm is also used after each generation to prevent two or more identical sensor locations (same integer value) to occur in the same population member.

The NSGA-II algorithm is applied in the Python environment using the Pymoo package (Blank and Deb 2020). The tuning process is carried out as described in 2.2 and it is based on an initial estimation of NSGAII parameters (see Table 1). This estimation is characterized by a default PS and NG of 100, as well as a simulated binary crossover (with high-probability $p_c = 0.95$ and default distribution indices $n_c = 10$), and a polynomial mutation (with low-probability $p_m = 0.05$ and default distribution indices $n_m = 10$). Furthermore, random sampling and selection methods are considered.

The first parameter to be tuned is the population size, PS. An unconstrained multi-objective optimization problem is formulated for 10 sensors (with the possible locations being the result of the search space reduction). Three distinct sets of parameters are used by considering the PS parameter equal to 50, 100, and 250, resulting in combinations of parameters C1, C2, and C3, respectively. The remaining parameters are used as in the initial set of parameters (see Table 1). The hypervolume indicator is used to assess the evolution of the Pareto front. The use of the hypervolume indicator differs from that explained in 2.3, in the sense that it is calculated for each generation (and not just for the final Pareto front). To account for the heuristic nature of the optimization algorithm, three distinct runs of each combination are carried out (i.e. each combination of parameters C1, C2, and C3 was used three times to solve the optimization problem). Each of these runs uses a particular sequence of random numbers (commonly known as seed), and which is the same across combinations. For example, the 1st, 2nd, and 3rd runs of the Combination C1 uses seed 1, 2 and 3, respectively. Similarly, the 1st, 2nd, and 3rd runs of the Combination C2 use seeds 1, 2 and 3. Figure 5 presents the obtained results for C1, C2 and C3, represented by three lines in red, green, or blue color. The computational times for a single run of the three combinations are 42, 82, and 201 s, respectively. All optimization problems presented herein are solved using an Intel Core i5-8250 U processor of 1.80 GHz and 8 GB of memory. This figure shows that a higher population size is preferable, as better results are obtained when using 100 or 250 individuals. The total number of OF evaluations is equal to the PS times the NG, so the PS has a direct impact on the total computational time. Since comparable results are obtained when considering either C2 or C3 (with PS of 100 and 250), the former is used herein, representing a reduction factor of 2.5 in the total computational time.

The second parameter to be tuned is the number of generations, NG. A similar tuning process is performed by considering three distinct values for the NG parameter, namely, 100, 250, and 1000 generations (resulting in combinations C4, C5, and C6, respectively). The tuned value of PS = 100 is used,

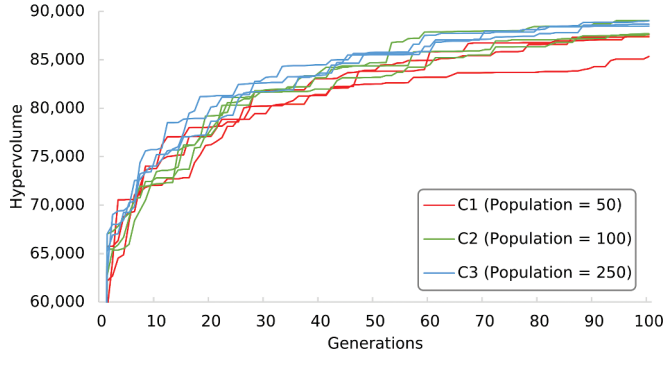

Figure 5. Hypervolume evolution across generations for different values of population size.

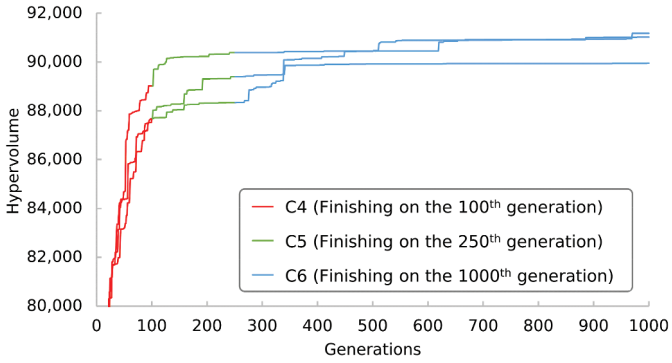

Figure 6. Hypervolume evolution across generations for three distinct runs.

while the remaining parameters are considered equal to those in the initial set of parameters (see Table 1). Figure 6 presents the obtained results for three different runs ending on the 100th, the 250th or the 1000th GA generation.

Indeed, a higher number of generations is better, with significant improvement in hypervolume indicator being observed at the 600th or 900th generation. These improvements suggest that even more than a thousand generations should be considered. Nonetheless, this higher number of generations is reflected in the total computational time, with C4, C5, and C6 taking, respectively, 82, 403, and 802 s. As such, an NG of 1000 is considered for the remaining tuning process, while a higher NG of 2,500 is considered for the actual case study.

The third parameter to be tuned is the crossover operator. A total of 15 combinations of parameters (by varying the crossover operator) were considered (combinations C7 to C22). Nine combinations (C7 to C15) are related to the SB operator since three values for p_c and three values for n_c were combined. Uniform, half-uniform, one-point, and two-point do not require internal parameters, thus resulting in just a single combination for each parameter (C16 to C19). Two combinations (C20 and C21) are considered for the exponential crossover operator by varying its internal parameter p. The tuned values of PS = 100 and NG = 1000 are used, while the mutation operator parameter is considered equal to those in the initial set of parameters (see Table 1). A similar tuning process is carried out, with three optimization problems being solved for each combination of parameters. The average of the three simulation runs for each combination of parameters is calculated and presented in Figure 7. Figure 7(a) presents the obtained results for nine combinations (C7 to C15) for the SB crossover operator, while Figure 7(b) presents the results for the remaining combinations (C16 to C21).

As expected, different values for probability p_c and distribution indices n_c in SB operator produce very distinct results (see Figure 7a). This operator, depending on the combination of p_c and n_c, leads to both the worst overall solution (C10) and the 2nd best overall solution (C15). The best results are obtained when considering a low probability of crossover p_c = 0.05 (C15 and C12). Furthermore, p_c seems to have a higher impact on NSGA-II performance than n_c; this can be seen in the results for two combinations C12 and C15, which differ greatly in the value of the distribution indices n_c (3 and 20) and produce the two best results for this particular crossover operator.

The results of the remaining crossover operators in Figure 7(b) show that uniform (C16) and exponential crossover with p equal to 0.95 (C20) presents the best overall results, with the highest hypervolume value in the 1,000th generation, as well as a high hypervolume value since early generations (300th generation for instance).

The best overall results are obtained by using either the SB with a specific combination of internal parameters (C15) or the uniform crossover operator (C16). The latter operator is preferable, since it does not contain internal parameters and will be used in the following tuning process of the mutation operator and in the actual case study.

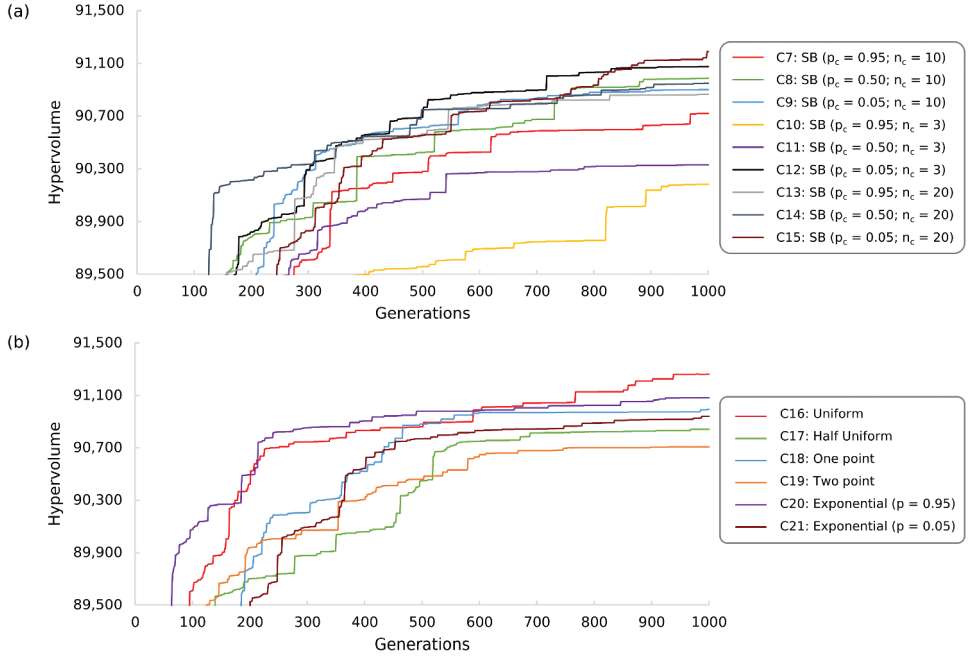

Figure 7. Hypervolume evolution across generations for different crossover operators.

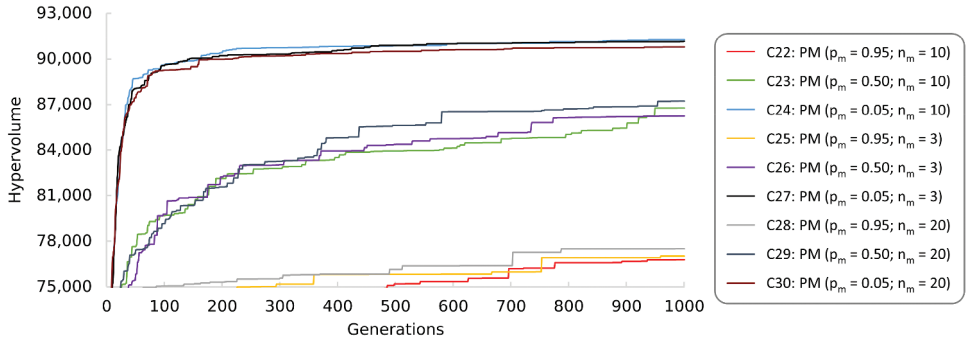

Figure 8. Hypervolume evolution across generations for different values of the polynomial mutation's parameters.

Table 3. NSGA-II parameters after tuning.

Parameter	After tuning
Population Size (PS)	100
Number of generations (NG)	1,000 (2,500)
Crossover operator	Uniform crossover
Mutation operator	Polynomial mutation (p_m=0.05; n_m=10)

The final parameter to be tuned is the mutation operator. Three distinct values are considered for p_m, namely, 0.05, 0.50, and 0.95. Similarly, three distinct values are considered for the n_m, namely, 3, 10, and 20. This leads to a total of nine combinations (C22 to C30). The tuned values of PS and NG are used, as well as the uniform crossover operator. The same tuning process is carried out, with three optimization problems being solved for each combination of parameters. The average of the three simulation runs for each combination of parameters is calculated and presented in Figure 8. Lower values of $p_m = 0.05$ are preferable, with significant differences being found for the three distinct values of p_m. Although the mutation operator is needed to skip the local search space, high mutation rates can lead the search to be random. Furthermore, p_m has a higher impact on NSGA-II performance than n_m; this can be seen by comparing the results of three combinations with similar p_m and distinct n_m (for instance, C23, C26, and C29) with three combinations with similar n_m and distinct p_m (for instance, C25, C26, and C27).

The best combinations of parameters are C24 and C27, both with $p_m = 0.05$ and with n_m of 10 and 3, respectively. So, the polynomial mutation operator with $p_m = 0.05$ and $n_m = 10$ is used for the case study. The final set of NSGA-II parameters after tuning is presented in Table 3.

3.3 Multi-objective optimization of pressure sensors' location

The minimum and maximum numbers of sensors, N_{min} and N_{max}, are defined, respectively, as 1 and 20 sensors. The latter is defined according to the water utility budget limitation. The unconstrained multi-objective problem is formulated as previously described and solved twenty times using the NSGA-II algorithm (Deb et al. 2002), one for each number of sensors, and by using the set of tuned NSGA-II

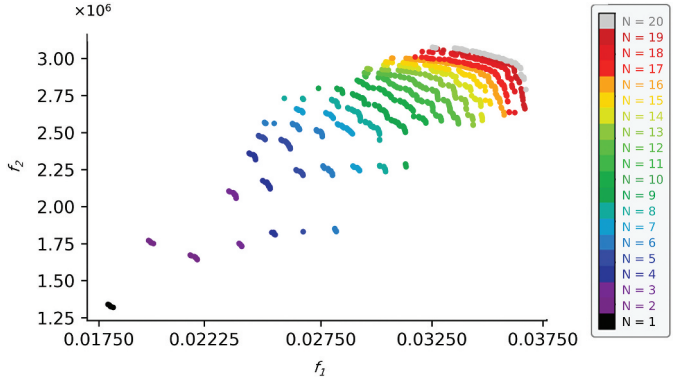

Figure 9. Obtained Pareto fronts.

parameters (see Table 3). The possible locations for pressure sensors are the result locations of the search space reduction. Each optimization problem is solved for 2,500 generations, resulting in $2{,}500 \times 100 = 250{,}000$ objective function evaluations, and with a total running time of around 35 min per optimization problem. The result of each optimization problem is a Pareto front of optimal pressure sensor locations (according to the objective functions f_1 and f_2). These Pareto fronts are depicted in Figure 9. Each dot represents a possible combination of a given number of sensors N between 1 and 20. The optimal combination for a given number of pressure sensors is not the same when individually maximizing each objective and there are several trade-off optimal solutions when attending to both objectives simultaneously. Furthermore, Pareto fronts for a higher number of pressure sensors (for instance, 19 and 20 sensors) appear to be 'closer' to each other than the Pareto fronts obtained for a lower number of pressure sensors (for instance, 1 and 2 sensors). This is expected since there is a greater marginal benefit of installing a second sensor than a 20th. This behavior should be assessed by the quality

measures when characterizing the total benefit associated with each number of pressure sensors (as assessed in the following section).

3.4 Optimal number of pressure sensors by using quality measures

Both the hypervolume and the adaptation of the generational distance indicators are calculated for each Pareto front as shown in Figure 9 (and as described in 2.3). The obtained results are depicted in Figure 10. The increase in the number of installed sensors leads to a higher benefit; this can be observed in Figure 10 with the highest hypervolume and the generational distance values being found for 20 sensors. Furthermore, the marginal benefit decreases for a higher number of pressure sensors; this behaviour is observed in both quality measures (besides the different order of magnitude). Nonetheless, the generational distance indicator appears to be susceptible to the shape of the Pareto front, as a higher marginal benefit is obtained from 6 to 7 sensors than it was obtained from 5 to 6 sensors. This is due to the sudden changes in the Pareto from 6 to 7 sensors (see Figure 9). The hypervolume, on the other hand, is not so susceptible to changes in the Pareto front and consecutively decreasing marginal benefits are obtained.

These results show that both quality measures (hypervolume and generational distance) can describe the total benefit of installing a different number of pressure sensors, though the former appears to be less influenced by the shape of the Pareto front.

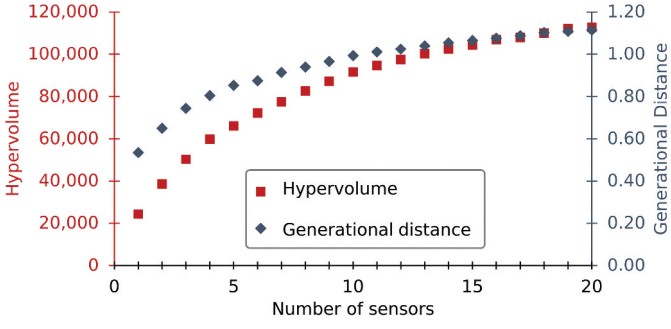

Figure 10. Hypervolume and generational distance for the different number of pressure sensors.

A cost–benefit analysis is used to determine the optimal number of pressure sensors N_{opt} by assessing the number of sensors with the maximum final net cost *NC*. A test is performed to assess if major differences in the optimal number of pressure sensors are found by considering either the hypervolume or the generational distance to quantify the benefit for each number of sensors. Two separate cost–benefit analyses are carried out, one by using the hypervolume and the other by using the generational distance. Both sets of hypervolume and generational distance values presented in Figure 10 are normalized into [0,1] (see 2.3), leading to HV_{norm} and GD_{norm} values. The former is depicted in Figure 11(a) as red squares, while the latter is presented in Figure 11(b) as blue diamonds. The total expenditure *TOTEX* is also normalized into [0,1] and depicted in Figure 11 as black circles. The final net cost *NC* for each number of sensors is calculated twice (using either HV_{norm} or GD_{norm}), leading to NC_{HV} and NC_{GD}, and is represented in Figure 11 as red or blue triangles, respectively.

Finally, the optimal number of sensors is found as the number of sensors with the maximum value of the net cost NC_{HV} and NC_{GD} (represented in a blue arrow); the former is found to be equal to 8 sensors, while the latter is equal to 7 sensors. No major difference in the optimal number of sensors is attained by using the hypervolume or the generational distance indicator. The hypervolume is recommended due to the previously presented characteristics, such as the simplicity and the ability to capture the spread of the Pareto fronts. The optimal number of pressure sensors N_{opt} is, thus, defined as 8 sensors.

Once the number of sensors is defined as 8, an optimal configuration can be chosen from the Pareto front (see Figure 9). Figure 12 presents the Pareto front for 8 sensors, where each grey point represents an optimal configuration. Three distinct configurations are highlighted: the configuration that maximizes the f_1 objective (in a red triangle), the solution that maximizes the f_2 objective (in a green triangle), and a trade-off solution between these two objectives (in a blue triangle).

Figure 13 depicts the location of these three highlighted configurations of 8 sensors in the WDN. This figure shows that the optimal location for pressure sensors depends strongly on the chosen solution of the Pareto front (i.e. either maximizing an objective or a trade-off solution). As a result, different optimal locations could be found for the solutions that individually maximize each objective (red and green triangles).

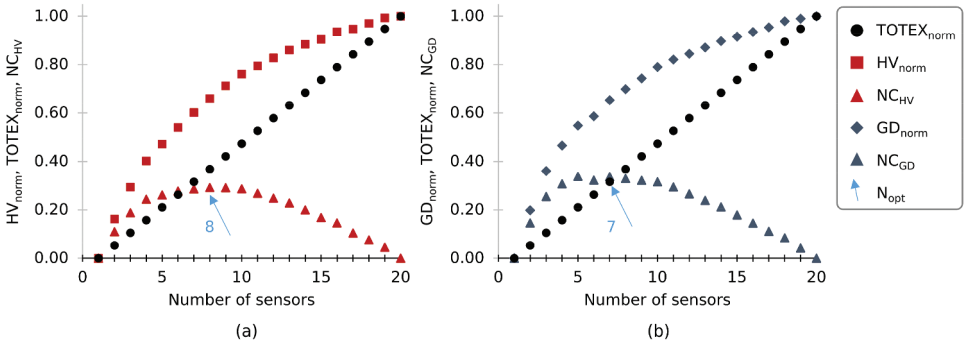

Figure 11. Optimal number of sensors using a cost-benefit analysis and by assessing the total benefit using: (a) the hypervolume; (b) the generational distance.

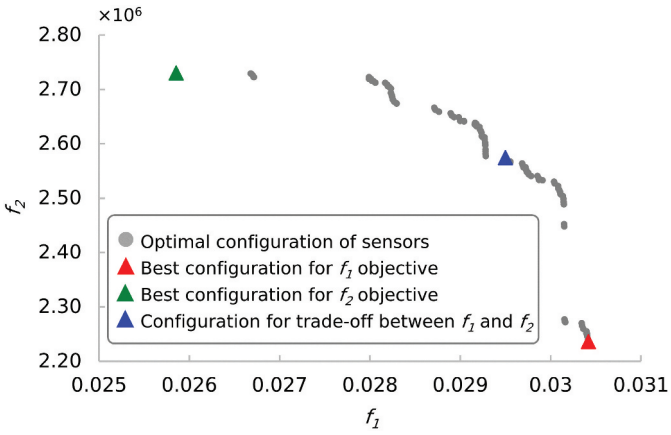

Figure 12. Pareto front for 8 sensors with three highlighted solutions.

As noted earlier, the maximization of sensitivities may lead to sensors clustered in zones with highly sensitive nodes. This can be seen in Figure 13, where two sensors are clustered in both f_1 and f_2 solutions (although in different zones of the WDN). The trade-off solution, which considersboth objectives simultaneous, results in more evenly spread sensor locations throughout the WDN. Summing up, the trade-off solution should be adopted as it contains compromised locations between f_1 and f_2 solutions in several network zones.

4. Conclusions

This paper presents an extensive analysis of NSGA-II parameterization for the optimal pressure sensor configuration for WDNs. A multi-objective optimization methodology is used to optimally locate a given number of pressure sensors. The location of pressure sensors is determined such that they can be used for the continuous calibration (in terms of pipe roughness coefficient) of the hydraulic model, as well as used to detect and locate pipe bursts. Two distinct OFs are formulated, maximizing nodal pressure sensitivities to both pipe roughness coefficients and pipe burst events. This ensures that pressure sensors are optimally located to generate pressure-head data to be used in the calibration of the hydraulic model and for pipe burst detection.

A total of 30 different combinations of NSGA-II parameters are considered by varying the population size, the number of generations, the crossover, and the mutation operator. These combinations are assessed by using the hypervolume indicator to measure the evolution of the Pareto front across the generations for each combination of parameters. Ninety multi-objective optimization problems are solved to find a suitable set of NSGA-II parameters. Results demonstrate that the population size should be appropriately selected as it has a direct influence on the total computation time; similar results are obtained when considering population sizes of 100 and 250, with the former representing a reduction factor of 2.5 in the total computational time. Simulated binary, depending on its internal parameters (with a total of 9 combinations), leads to both the second best and the overall worst results when tuning the crossover operator. On the other hand, the uniform crossover operator produces the best overall results and it does not require internal parameters to be defined. So, the uniform crossover operator is therefore recommended. A polynomial mutation operator with lower probability values is preferable (i.e. 0.05), with significant differences being found for the two other analyzed values (0.50 and 0.95). The distribution indices of the polynomial mutations have a minor effect on NSGA-II performance.

The optimal number of pressure sensors is determined by using a cost–benefit analysis. An unconstrained multi-objective optimization problem is formulated and solved (using the tuned set of parameters) for a range of between 1 and 20 pressure sensors. The benefit of installing each number of sensors is assessed by using two distinct quality measures, namely, the hypervolume and an adaption of the generational distance. The objective is to assess if major differences in the optimal number of pressure sensors exist by using different quality measures. No differences have been observed, being the optimal number of pressure sensors found by using the

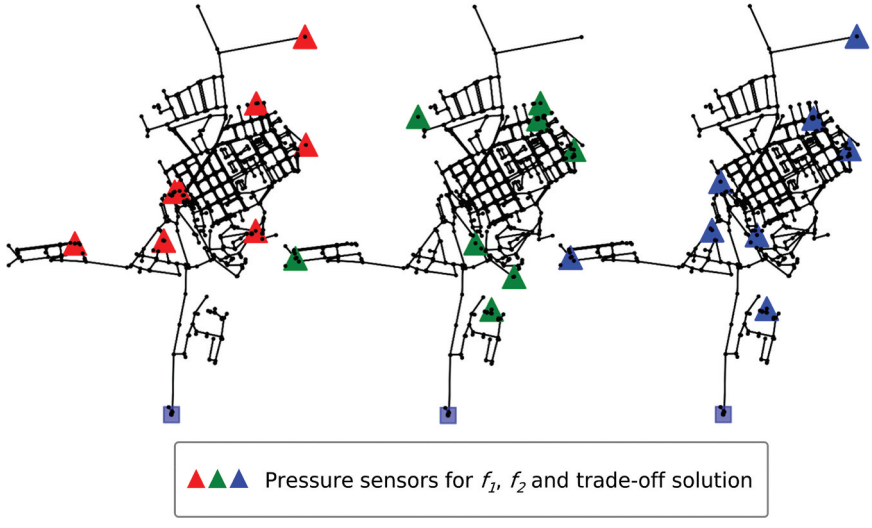

Figure 13. Optimal pressure sensor location of the three highlighted solutions.

hypervolume and the generational distance being equal to 8 and 7, respectively. The hypervolume is herein recommended due to its characteristics, such as the simplicity and the ability to capture the spread of the Pareto fronts (as opposed to the generational distance which could only capture the average distance of the set of solutions to the reference point).

Finally, the results have demonstrated the importance of using tools, such as optimization techniques, to help water utilities to address real-life problems, which are often too complex to be solved solely by engineering judgment. The use of such tools allows utilities to explore a higher number of solutions and, ultimately, increase the benefit of installing pressure sensors. Nonetheless, the experts' judgment is crucial for the correct use of such tools, not only in the problem formulation but also in the critical analysis of the obtained results.

Acknowledgements

The authors would like to thank the Fundação para a Ciência e Tecnologia (FCT) for funding this research and the water utility for providing the case study and the data.

Disclosure statement

No potential conflict of interest was reported by the authors.

Funding

This work was supported by the Fundação para a Ciência e a Tecnologia through the WISDom project (grant number DSAIPA/DS/0089/2018), the PhD. Research Studentship of Bruno Ferreira (grant number SFRH/BD/149392/2019), and the research unit CERIS (grant number UIDB/04625/2020)

ORCID

Bruno Ferreira http://orcid.org/0000-0002-2863-7949
André Antunes http://orcid.org/0000-0001-9030-5956
Nelson Carriço http://orcid.org/0000-0002-2474-7665
Dídia Covas http://orcid.org/0000-0001-6901-4767

Data availability statement

The data presented in this study are available on request from the corresponding author. The data are not publicly available due to being obtained from third parties.

Author contributions

B.F. and A.A. designed and developed the methodology; B.F. analyzed the data and drafted the manuscript; N.C. and D.C. guided and supervised the whole process; N.C. and D.C. revised the manuscript; and all authors read and approved the final manuscript.

References

Audet, C., J. Bigeon, D. Cartier, S. Le Digabel, and L. Salomon. 2021. "Performance Indicators in Multiobjective Optimization." *European Journal of Operational Research* 292 (2): 397–422. doi:10.1016/j.ejor.2020.11.016.

Auger, A., J. Bader, D. Brockhoff, and E. Zitzler 2009. "Theory of the Hypervolume Indicator". *Proceedings of the Tenth ACM SIGEVO Workshop on Foundations of Genetic Algorithms - FOGA '09*, 87. 10.1145/1527125.1527138

Behzadian, K., Z. Kapelan, D. Savic, and A. Ardeshir. 2009. "Stochastic Sampling Design Using a Multi-Objective Genetic Algorithm and Adaptive Neural Networks." *Environmental Modelling & Software* 24 (4): 530–541. doi:10.1016/j.envsoft.2008.09.013.

Blank, J., and K. Deb. 2020. "Pymoo: Multi-Objective Optimization in Python." *Institute of Electrical and Electronics EngineersAccess* 8: 89497–89509. doi:10.1109/ACCESS.2020.2990567.

Cao, H., S. Hopfgarten, A. Ostfeld, E. Salomons, and P. Li. 2019. "Simultaneous Sensor Placement and Pressure Reducing Valve Localization for Pressure Control of Water Distribution Systems." *Water (Switzerland)* 11 (7): 1352. doi:10.3390/w11071352.

Capelo, M., B. Brentan, L. Monteiro, and D. Covas. 2021. "Near–Real Time Burst Location and Sizing in Water Distribution Systems Using Artificial Neural Networks." *Water* 13 (13): 1841. doi:10.3390/w13131841.

Casillas, M., V. Puig, L. Garza-Castañón, and A. Rosich. 2013. "Optimal Sensor Placement for Leak Location in Water Distribution Networks Using Genetic Algorithms." *Sensors* 13 (11): 14984–15005. doi:10.3390/s131114984.

Coello Coello, C. A., and M. S. Lechuga. 2002. "MOPSO: A Proposal for Multiple Objective Particle Swarm Optimization." *Current Topics in Medicinal Chemistry* 2 (9): 1051–1056. *Proceedings of the 2002 Congress on Evolutionary Computation. CEC'02 (Cat. No.02TH8600)*. doi:10.1109/CEC.2002.1004388.

Deb, K., A. Pratap, S. Agarwal, and T. Meyarivan. 2002. "A Fast and Elitist Multiobjective Genetic Algorithm: NSGA-II." *IEEE Transactions on Evolutionary Computation* 6 (2): 182–197. doi:10.1109/4235.996017.

Deb, K., K. Sindhya, and T. Okabe 2007. "Self-Adaptive Simulated Binary Crossover for Real-Parameter Optimization". *Proceedings of GECCO 2007: Genetic and Evolutionary Computation Conference*, 1187–1194. 10.1145/1276958.1277190

Dini, M., and M. Tabesh. 2014. "A New Method for Simultaneous Calibration of Demand Pattern and Hazen-Williams Coefficients in Water Distribution Systems." *Water Resources Management* 28 (7): 2021–2034. doi:10.1007/s11269-014-0592-4.

Do, N. C., A. R. Simpson, J. W. Deuerlein, and O. Piller. 2016. "Calibration of Water Demand Multipliers in Water Distribution Systems Using Genetic Algorithms." *Journal of Water Resources Planning and Management* 142 (11): 1–13. doi:10.1061/(ASCE)WR.1943-5452.0000691.

Fereidooni, Z., H. Tahayori, and A. Bahadori-Jahromi. 2021. "A Hybrid Model-Based Method for Leak Detection in Large Scale Water Distribution Networks." *Journal of Ambient Intelligence and Humanized Computing* 12 (2): 1613–1629. doi:10.1007/s12652-020-02233-2.

Ferreira, B., A. Antunes, N. Carriço, and D. Covas. 2022. "Multi-Objective Optimization of Pressure Sensor Location for Burst Detection and Network Calibration." *Computers & Chemical Engineering* 162: 107826. doi:10.1016/j.compchemeng.2022.107826.

Ferreira, B., N. Carriço, and D. Covas. 2021. "Optimal Number of Pressure Sensors for Real-Time Monitoring of Distribution Networks by Using the Hypervolume Indicator." *Water* 13 (16): 2235. doi:10.3390/w13162235.

Fonseca, C. M., and P. Fleming. 1993. "Genetic Algorithms for Multiobjective Optimization: Formulation, Discussion and Generalization." *Igca* 93 (July): 416–423.

Francés-Chust, J., B. M. Brentan, S. Carpitella, J. Izquierdo, and I. Montalvo. 2020. "Optimal Placement of Pressure Sensors Using Fuzzy DEMATEL-Based Sensor Influence." *Water* 12 (2): 493. doi:10.3390/w12020493.

Gomes, S. C., S. Vinga, and R. Henriques. 2021. "Spatiotemporal Correlation Feature Spaces to Support Anomaly Detection in Water Distribution Networks." *Water* 13 (18): 2551. doi:10.3390/w13182551.

Goulet, J.-A., S. Coutu, and I. F. C. Smith. 2013. "Model Falsification Diagnosis and Sensor Placement for Leak Detection in Pressurized Pipe Networks." *Advanced Engineering Informatics* 27 (2): 261–269. doi:10.1016/j.aei.2013.01.001.

Guerreiro, A. P., C. M. Fonseca, and L. Paquete. 2020. "The Hypervolume Indicator: Problems and Algorithms." *ArXiv*.

Hajibandeh, E., and S. Nazif. 2018. "Pressure Zoning Approach for Leak Detection in Water Distribution Systems Based on a Multi Objective

Ant Colony Optimization." *Water Resources Management* 32 (7): 2287–2300. doi:10.1007/s11269-018-1929-1.

Hu, Z., W. Chen, B. Chen, D. Tan, Y. Zhang, and D. Shen. 2021. "Robust Hierarchical Sensor Optimization Placement Method for Leak Detection in Water Distribution System." *Water Resources Management* 35 (12): 3995–4008. doi:10.1007/s11269-021-02922-3.

Hu, X., Y. Han, B. Yu, Z. Geng, and J. Fan. 2021. "Novel Leakage Detection and Water Loss Management of Urban Water Supply Network Using Multiscale Neural Networks." *Journal of Cleaner Production* 278: 123611. doi:10.1016/j.jclepro.2020.123611.

Kapelan, Z. S., D. A. Savic, and G. A. Walterrs. 2007. "Calibration of Water Distribution Hydraulic Models Using a Bayesian-Type Procedure." *Journal of Hydraulic Engineering* 133 (8): 927–936. doi:10.1061/(ASCE)0733-9429(2007)133:8(927).

Kapelan, Z. S., D. A. Savic, and G. A. Walters. 2005. "Optimal Sampling Design Methodologies for Water Distribution Model Calibration." *Journal of Hydraulic Engineering* 131 (3): 190–200. doi:10.1061/(ASCE)0733-9429(2005)131:3(190).

Klapcsik, K., R. Varga, and C. Hős. 2017. "Optimal Pressure Measurement Layout Design in Water Distribution Network Systems." *Periodica Polytechnica Mechanical Engineering* 62 (1): 51. doi:10.3311/PPme.11409.

Klise, K. A., M. Bynum, D. Moriarty, and R. Murray. 2017. "A Software Framework for Assessing the Resilience of Drinking Water Systems to Disasters with an Example Earthquake Case Study." *Environmental Modelling & Software* 95: 420–431. doi:10.1016/j.envsoft.2017.06.022.

Kumar, S. M., S. Narasimhan, and S. M. Bhallamudi. 2010. "Parameter Estimation in Water Distribution Networks." *Water Resources Management* 24 (6): 1251–1272. doi:10.1007/s11269-009-9495-1.

Laszczyk, M., and P. B. Myszkowski. 2019. "Survey of Quality Measures for Multi-Objective Optimization: Construction of Complementary Set of Multi-Objective Quality Measures." *Swarm and Evolutionary Computation* 48: 109–133. doi:10.1016/j.swevo.2019.04.001.

Leitão, J. P., S. T. Coelho, H. Alegre, M. A. Cardoso, M. S. Silva, P. Ramalho, R. Ribeiro, et al. 2016. "Moving Urban Water Infrastructure Asset Management from Science into Practice." *Urban Water Journal* 13 (2): 133–141. doi:10.1080/1573062X.2014.939092.

Liggett, J. A., and L. Chen. 1994. "Inverse Transient Analysis in Pipe Networks." *Journal of Hydraulic Engineering* 120 (8): 934–955. doi:10.1061/(ASCE)0733-9429(1994)120:8(934).

Maier, H. R., Z. Kapelan, J. Kasprzyk, J. Kollat, L. S. Matott, M. C. Cunha, G. C. Dandy. 2014. "Evolutionary Algorithms and Other Metaheuristics in Water Resources: Current Status, Research Challenges and Future Directions." *Environmental Modelling and Software* 62: 271–299. doi:10.1016/j.envsoft.2014.09.013.

Mala-Jetmarova, H., N. Sultanova, and D. Savic. 2018. "Lost in Optimisation of Water Distribution Systems? A Literature Review of System Design." *Water* 10 (3): 307. doi:10.3390/w10030307.

Meirelles, G., D. Manzi, B. Brentan, T. Goulart, and E. Luvizotto. 2017. "Calibration Model for Water Distribution Network Using Pressures Estimated by Artificial Neural Networks." *Water Resources Management* 31 (13): 4339–4351. doi:10.1007/s11269-017-1750-2.

Menke, R., E. Abraham, P. Parpas, and I. Stoianov. 2016. "Exploring Optimal Pump Scheduling in Water Distribution Networks with Branch and Bound Methods." *Water Resources Management* 30 (14): 5333–5349. doi:10.1007/s11269-016-1490-8.

Moasheri, R., and M. Jalili-Ghazizadeh. 2020. "Locating of Probabilistic Leakage Areas in Water Distribution Networks by a Calibration Method Using the Imperialist Competitive Algorithm." *Water Resources Management* 34 (1): 35–49. doi:10.1007/s11269-019-02388-4.

Moser, G., S. G. Paal, and I. F. C. Smith. 2018. "Leak Detection of Water Supply Networks Using Error-Domain Model Falsification." *Journal of Computing in Civil Engineering* 32 (2): 04017077. doi:10.1061/(ASCE)CP.1943-5487.0000729.

Pérez, R., V. Puig, J. Pascual, J. Quevedo, E. Landeros, and A. Peralta. 2011. "Methodology for Leakage Isolation Using Pressure Sensitivity Analysis in Water Distribution Networks." *Control Engineering Practice* 19 (10): 1157–1167. doi:10.1016/j.conengprac.2011.06.004.

Quintiliani, C., I. Vertommen, K. Laarhoven, Vliet van, J. van der, and P. van Thienen. 2020. "Optimal Pressure Sensor Locations for Leak Detection in a Dutch Water Distribution Network." *Environmental Sciences Proceedings* 2 (1): 40. doi:10.3390/environsciproc2020002040.

Raei, E., M. E. Shafiee, M. R. Nikoo, and E. Berglund. 2019. "Placing an Ensemble of Pressure Sensors for Leak Detection in Water Distribution Networks Under Measurement Uncertainty." *Journal of Hydroinformatics* 21 (2): 223–239. doi:10.2166/hydro.2018.032.

Rayaroth, R., and S. G. 2019. "Random Bagging Classifier and Shuffled Frog Leaping Based Optimal Sensor Placement for Leakage Detection in WDS." *Water Resources Management* 33 (9): 3111–3125. doi:10.1007/s11269-019-02296-7.

Reed, P. M., D. Hadka, J. D. Herman, J. R. Kasprzyk, and J. B. Kollat. 2013. "Evolutionary Multiobjective Optimization in Water Resources: The Past, Present, and Future." *Advances in Water Resources* 51: 438–456. doi:10.1016/j.advwatres.2012.01.005.

Rossman, L. 2000. *EPANET 2 User's Manual (Issue September)*. Washington, DC, USA: United States Environmental Protection Agency.

Salloom, T., O. Kaynak, and W. He. 2021. "A Novel Deep Neural Network Architecture for Real-Time Water Demand Forecasting." *Journal of Hydrology* 599 (April): 126353. doi:10.1016/j.jhydrol.2021.126353.

Sarrate, R., J. Blesa, F. Nejjari, and J. Quevedo. 2014. "Sensor Placement for Leak Detection and Location in Water Distribution Networks." *Water Supply* 14 (5): 795–803. doi:10.2166/ws.2014.037.

Simone, A., O. Giustolisi, and D. B. Laucelli. 2016. "A Proposal of Optimal Sampling Design Using a Modularity Strategy." *Water Resources Research* 52 (8): 6171–6185. doi:10.1002/2016WR018944.

Sophocleous, S., D. Savić, and Z. Kapelan. 2019. "Leak Localization in a Real Water Distribution Network Based on Search-Space Reduction." *Journal of Water Resources Planning and Management* 145 (7): 04019024. doi:10.1061/(ASCE)WR.1943-5452.0001079.

Steffelbauer, D. B., and D. Fuchs-Hanusch. 2016. "Efficient Sensor Placement for Leak Localization Considering Uncertainties." *Water Resources Management* 30 (14): 5517–5533. doi:10.1007/s11269-016-1504-6.

Van Veldhuizen, D. 1999. *Multiobjective Evolutionary Algorithms: Classifications, Analyses, and New Innovations*. Dayton, OH: Air Force Institute of Technology.

Vonk, E., Cirkel D., Blokker, M. 2019. "Estimating Peak Daily Water Demand Under Different Climate Change and Vacation Scenarios." *Water* 11 (9): 1874. doi:10.3390/w11091874.

Wang, Q., L. Wang, W. Huang, Z. Wang, S. Liu, and D. A. Savić. 2019. "Parameterization of NSGA-II for the Optimal Design of Water Distribution Systems." *Water* 11 (5): 971. doi:10.3390/w11050971.

While, L., P. Hingston, L. Barone, and S. Huband. 2006. "A Faster Algorithm for Calculating Hypervolume." *IEEE Transactions on Evolutionary Computation* 10 (1): 29–38. doi:10.1109/TEVC.2005.851275.

Wolpert, D. H., and W. G. Macready. 1997. "No Free Lunch Theorems for Optimization." *IEEE Transactions on Evolutionary Computation* 1 (1): 67–82. doi:10.1109/4235.585893.

Zhang, Q., F. Zheng, H.-F. Duan, Y. Jia, T. Zhang, and X. Guo. 2018. "Efficient Numerical Approach for Simultaneous Calibration of Pipe Roughness Coefficients and Nodal Demands for Water Distribution Systems." *Journal of Water Resources Planning and Management* 144 (10): 04018063. doi:10.1061/(ASCE)WR.1943-5452.0000986.

Zhao, M., C. Zhang, H. Liu, G. Fu, and Y. Wang. 2020. "Optimal Sensor Placement for Pipe Burst Detection in Water Distribution Systems Using Cost–Benefit Analysis." *Journal of Hydroinformatics* 22 (3): 606–618. doi:10.2166/hydro.2020.158.